Hydrometallurgy, 17 (1987) 369–384
Elsevier Science Publishers B.V., Amsterdam — Printed in The Netherlands

Kinetics and Mechanisms of the Non-oxidative Dissolution of Sphalerite (Zinc Sulphide)

F.K. CRUNDWELL and B. VERBAAN

MINTEK Hydrometallurgical Research Group, Department of Chemical Engineering, University of the Witwatersrand, Randburg 2125 (South Africa)

(Received March 17, 1986; accepted in revised form September 29, 1986)

ABSTRACT

Crundwell, F.K. and Verbaan, B., 1987. Kinetics and mechanisms of the non-oxidative dissolution of sphalerite (zinc sulphide). *Hydrometallurgy*, 17: 369–384.

The kinetics of the non-oxidative dissolution of four samples of sphalerite (ZnS) of different origin were studied. It was concluded that the dissolution is independent of the stirrer speed and is first order in $[H^+]$, and that the activation energies for the removal and deposition reactions are not sensitive to the impurity content of the solid. The rate of reaction is described by an ionic charge transfer mechanism. A large addition of Zn^{2+} retards the initial rate because equilibrium conditions are established, whereas the addition of H_2S to the reaction system lowers the final extent of reaction. The addition of Fe(III) retards the initial rate of reaction due to an anodic shift in the potential difference at the surface–solution interface, but increases the final extent of reaction as a result of the consumption of H_2S by Fe(III) to form elemental sulphur and Fe(II). The observed inhibition of the initial rate for the impure samples is explained in terms of an electron-transfer theory similar to that proposed for non-stoichiometric metal sulphides.

INTRODUCTION

The rate of dissolution of a solid, such as sphalerite, in aqueous solutions depends on the processes occurring at the solid–solution phase boundary. These processes include, amongst others, the formation of complexes, the transfer of charged species, and the adsorption of ions at the surface. The dissolution process can be classified on the basis of the rate-determining step, for example crystallization, mass transport, chemical reaction, or charge transfer [1].

Dissolution reactions can be further classified on the basis of the overall reaction into non-oxidative dissolution, in which no change in the formal oxidation state of the constituent atoms of the solid occurs, or oxidative or reductive dissolution, in which such a change does occur. For ionic solids, dissolution that involves the transfer of ions across the electrical double layer is classified as a chemical non-oxidative reaction, whereas, for predominantly covalent sol-

0304-386X/87/$03.50

ids, some form of electron-charge transfer may be rate-controlling, which would be classified as an electrochemical oxidative or reductive reaction [2].

The kinetics of non-oxidative dissolution reactions can be described by the use of either an empirical approach or a more fundamental approach in which the results are interpreted in terms of a model that includes a consideration of the electrochemical properties of the solid–solution phase boundary. It is common in hydrometallurgical studies to apply adsorption isotherms to the discussion of reaction kinetics. The adsorption of hydrogen ions on sulphur sites was proposed by Locker and DeBruyn [3] to account for the orders of reaction they observed in their study of the non-oxidative dissolution of group II–VI semiconductors. These findings were consistent with those of Romankiw and DeBruyn [4], which were obtained by a regression technique. Those isotherms make no provision for the effects of the electrical double layer and for the changes in the electrochemical potentials of the adsorbed ions — effects that are incorporated in an ionic charge-transfer theory.

Vermilyea [5] and Engell [6] proposed that the transfer of charged species across the electrochemical potential barrier at the solid–solution phase boundary controls the rate of dissolution. The main features of that theory are as follows: (i) the rates of transfer of anions and cations are exponentially dependent on the potential difference between the mineral surface and the outer Helmholtz plane, (ii) the transfer of cations and anions can be treated as independent processes, (iii) at steady state, the rates of transfer of cations and anions are equal, and (iv) the rate equation for each process at the 'freely-dissolving potential' can be combined in a way that is analogous to the mixed-potential model for corrosion. Diggle [2] has discussed the application of this theory to a number of metal oxides, and Nicol [7] has applied it to the leaching of metal sulphides.

For a dissolving semiconductor, such as sphalerite, a significant portion of the electrical double layer may include space-charge effects within the solid. Locker and DeBruyn [3] reported that the rate of non-oxidative dissolution of ZnS is controlled by the adsorption of hydrogen ions to the surface rather than by charge carriers in the solid. This is confirmed by the observation of Pawlek [8] that ultraviolet radiation does not substantially increase the rate of reaction.

DeBruyn and co-workers [3,4] described the non-oxidative dissolution of ZnS,

$$ZnS + H_2SO_4 \rightleftharpoons ZnSO_4 + H_2S \qquad (1)$$

in the concentration range 0.25 M to 10 M H_2SO_4 and temperature range 0.6 to 65 °C by the relation

$$\frac{d[Zn^{2+}]}{dt} = A_o\{k_1[H_2SO_4] - k_{-1}[ZnSO_4]^{0.5}p(H_2S)^{0.5}\} \qquad (2)$$

where A_o is the total initial area, k_1 and k_{-1} are rate constants, the brackets indicate concentration. They found that the kinetics of the non-oxidative dissolution of other group II–VI semiconductor compounds, such as ZnSe, CdS and $Zn_{0.85}Cd_{0.15}S$, are described by the same kinetic expression as that for ZnS, eqn. (2).

Locker and DeBruyn [3] excluded diffusion control, and proposed that the initial rate was controlled by the adsorption of protons at sulphur sites. They commented that when hydrochloric acid was used as the solvent, there was a possibility that specific adsorption of chloride ion would occur, which would change the surface charge and the distribution of active sites.

Recently, Majima et al. [9] observed that not only was the rate first order with respect to $[H^+]$, but the addition of NaCl to acidic chloride solutions also enhanced the rate of dissolution. They proposed an adsorption model similar to that of Locker and DeBruyn [3] to account for their results, but failed to explain the effect of the chloride ion.

The present study explores an electrochemical model for the non-oxidative dissolution of ZnS. However, since attempts by Scott and Nicol [10] to construct an electrode were not successful (owing to the high resistivity of ZnS), mechanisms are inferred from dissolution kinetics and the results are compared with those reported for other metal sulphides.

EXPERIMENTAL

Materials

Four sphalerite samples were used in this study: a pure natural sample from Ward's Scientific Museum (Ward's), a synthetic product (B.D.H.), and two impure natural sphalerites of South African origin, which are designated ZCR (Zincor) and PR (Prieska), respectively. The chemical composition of these samples is shown in Table 1.

Size reduction was effected by ball or vibratory (attrition) milling of the sample. The vibratory-milled impure sphalerites are designated VMZCR and VMPR. The pure natural sphalerite designated Ward's is vibratory-milled material. The specific surface areas of the various samples is shown in Table 1. Experiments on a closely sized fraction of Ward's material indicated that the mode of milling did not affect the dissolution characteristics beyond that due to size reduction. The natural sphalerites were pre-treated in dilute acid to remove any possible oxide layers or flotation reagents.

Etching studies were performed with concentrated sulphuric acid on mounted, polished sphalerite particles. Dissolution of the Ward's sample, in which no distinctive mineralogical features were observed, appeared to take place evenly over the entire surface. The ZCR sample etched in a complex manner, mainly along grain boundaries. The iron impurity of the PR sample

TABLE 1

Chemical composition of sphalerite samples (All values expressed in percentages)

	Natural pure (Ward's)	Synthetic pure (B.D.H.)	Natural impure (VMPR or PR)	Natural impure (VMZCR or ZCR)
Zn	66.5	66.2	52.1	56.7
S	32.2	32.6	32.9	32.6
Fe	0.45	0.12	10.74	7.25
Cu	0.038	0.013	3.53	0.016
Pb	0.090	0.056	0.085	1.51
Cd	0.48	0.008	0.13	0.12
Ni	0.040	0.041	0.050	0.041
Mg	0.023	0.040	0.17	0.36
Ca	0.035	0.027	0.1	0.63
Co	0.023	0.024	0.016	0.024
BET surface area (m^2/g)	3.27	7.2	2.63	2.71

was present in the sphalerite lattice, as well as in exsolved chalcopyrite. Iron-free sphalerite was observed to exist immediately adjacent to the chalcopyrite, the iron concentration increasing with distance from the chalcopyrite. Upon etching, preferential dissolution took place in the pure zones adjacent to the chalcopyrite.

Apparatus and procedure

The reactor consisted of a one litre spherical glass bowl, with a flat polyvinyl chloride top. Agitation was maintained by a titanium shaft and impeller driven by a variable speed motor. The stirrer speed was monitored with a 0 to 10000 min^{-1} tachometer. A single perspex baffle was installed. The total internal volume of the reactor with the top, impeller, baffle and measuring instruments installed was 1.35 litres.

A detailed description of the apparatus has been given elsewhere [11]. Temperature was maintained to within 0.25 °C by an 'Isopad' heating unit. A pressure transducer monitored the increase in pressure due to the evolution of H_2S, and this was recorded continuously on a chart recorder. The pressure transducer was calibrated with a mercury manometer. Care was taken to prevent gas leakage.

Accurate measurement of the initial rate of increase in pressure due to H_2S evolution was important, and increases due to the introduction of solids was minimised by using an adapted syringe as a plunger. Samples of ZnS of between 2 and 10 g for B.D.H. and 5 and 20 g for the others were introduced by a plunger

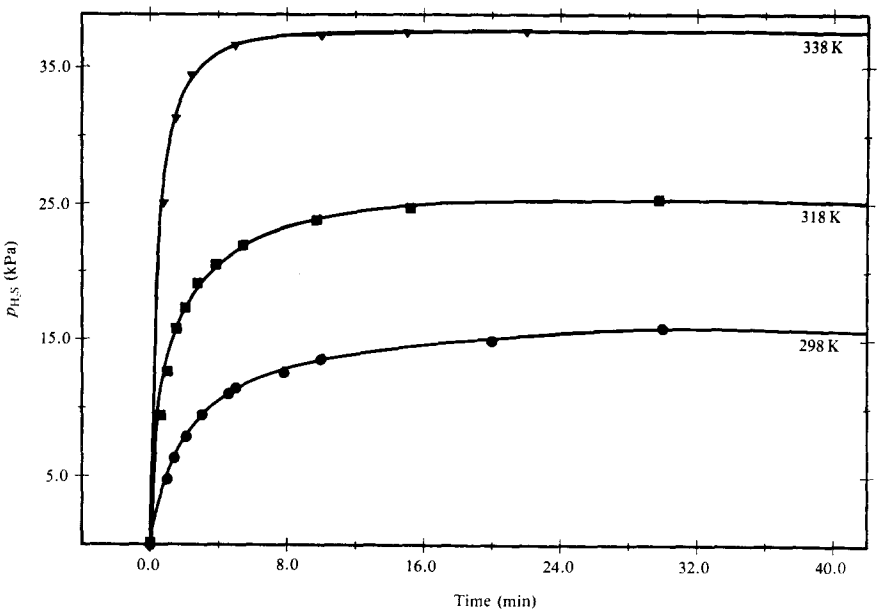

Fig. 1. Effect of temperature on dissolution of Ward's sphalerite in 1 M H_2SO_4 at a stirrer speed of 1000 min^{-1} (20 g ZnS/l).

to one litre of aqueous sulphuric acid solution once initial steady-state conditions had been attained. Samples of solution (5 ml) were taken at regular intervals with a hypodermic syringe and needle. A self-sealing rubber septum was fitted for this purpose. The samples were filtered immediately under vacuum.

The concentrations of zinc and iron in solution samples were determined by use of an atomic absorption spectrophotometer, and the concentration of acid was determined by titration with sodium carbonate, after the reduction of any Fe(III) in solution.

RESULTS

The initial rate of reaction at a stirrer speed of 400 min^{-1} was 0.047 mmol/m^2 min (298 K, 1 M H_2SO_4) for the B.D.H. sphalerite and the initial rate at stirrer speeds of 700 and 1000 min^{-1} was 0.062 mmol/m^2 min. The initial rates for the natural samples had a similar dependence on the stirrer speed. On the basis of this, a stirrer speed of 1000 min^{-1} was used in all subsequent experiments. This indicates that dissolution at stirrer speeds of 1000 min^{-1} is not diffusion controlled.

Typical kinetic results collected in the present study are presented in Fig. 1, which illustrates that an increase in temperature has a large effect on the rate of dissolution. All figures illustrating the increase of pressure with reaction

time represent the continuous chart recorder output, and the points on these figures represent times at which solution samples were taken.

If it is assumed that dissolution is controlled by a surface reaction in which the acid is the reactant, then, following Romankiw and DeBruyn [4],

$$r=\frac{1}{A}\frac{dn}{dt}=k_1[H^+]^{\alpha}-k_{-1}[Zn^{2+}]^{\beta}p(H_2S)^{\gamma} \quad (3)$$

where A is the surface area, n is the number of moles of H_2S or Zn^{2+} produced, and α, β and γ are coefficients.

The number of moles of solid dissolved was calculated from the measured H_2S partial pressure from

$$n=p(H_2S)\ V_1(1/K_D+V_g/RTV_1) \quad (4)$$

where $K_D=p(H_2S)/[H_2S]_{aq}$, V_g is the gas volume and V_1 is the liquid volume, and T is the temperature. The derivation of eqn. (4), presented elsewhere [4,11], assumes that $[H_2S]_{aq}$ is in equilibrium with $p(H_2S)$ (Henry's law) and that H_2S behaves like an ideal gas. The initial rate was determined by

$$r_o=\frac{1}{A}\left[\frac{dn}{dt}\right]_o=\frac{V_1}{A}\left[\frac{dp(H_2S)}{dt}\right]_o\{1/K_D+V_g/RTV_1\} \quad (5)$$

The derivative term $(dp(H_2S)/dt)_o$ was determined graphically from the chart recorder traces of the H_2S pressure and by a non-linear regression technique using numerous points selected from the H_2S pressure data [11]. The non-linear regression technique was similar to that used by Romankiw and DeBruyn [4]. The initial rate was then calculated using eqn. (5). The dissolution of the Fe and Cu components in the PR and ZCR samples would lead to evolution of H_2S not attributable to Zn, and therefore a minor deviation from eqn. (5).

The effect of the acid concentration was determined from a plot of the initial rate of reaction as a function of the H_2SO_4 concentration. This graph for the Ward's and the B.D.H. sphalerites is shown in Fig. 2, from which it is concluded that the rate is first order in H_2SO_4. This was also found to be true for the VMZCR and VMPR sphalerites.

The activation energy for the forward reaction was determined by plotting the logarithm of the initial rate, $\log r_o$, against $1/T$, as shown in Fig. 3. From this illustration it is concluded that the level of impurity in the solid sample does not significantly influence the activation energy.

Figures 4 and 5 show the effect of $p(H_2S)_o$ and $[Zn^{2+}]_o$ on the rate of dissolution, where $\Delta p(H_2S)$ is the increase in H_2S pressure above $p(H_2S)_o$. At equilibrium, the rate of the removal reaction is equal to the rate of the depo-

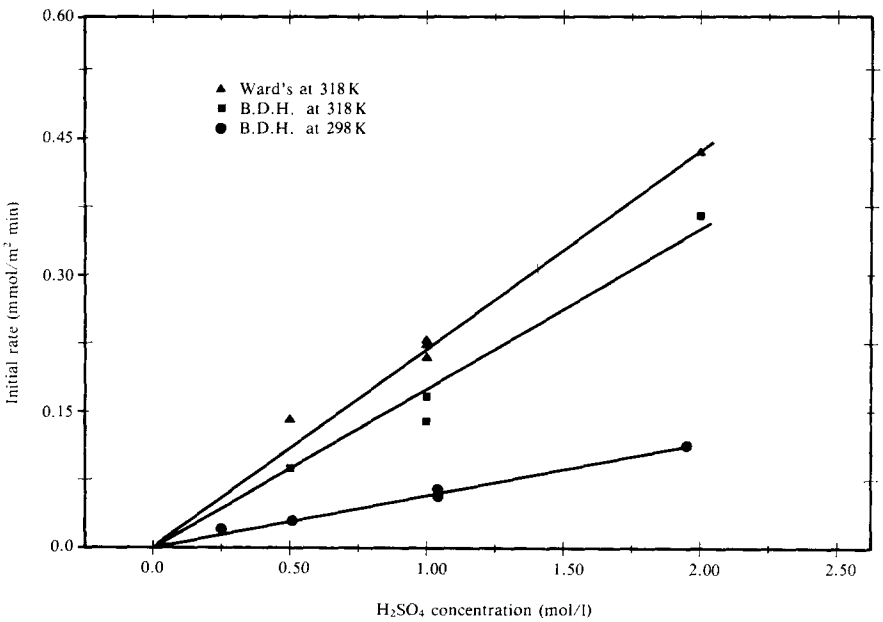

Fig. 2. Effect of H_2SO_4 concentration on dissolution of Ward's and B.D.H. samples at a stirrer speed of 1000 min^{-1}.

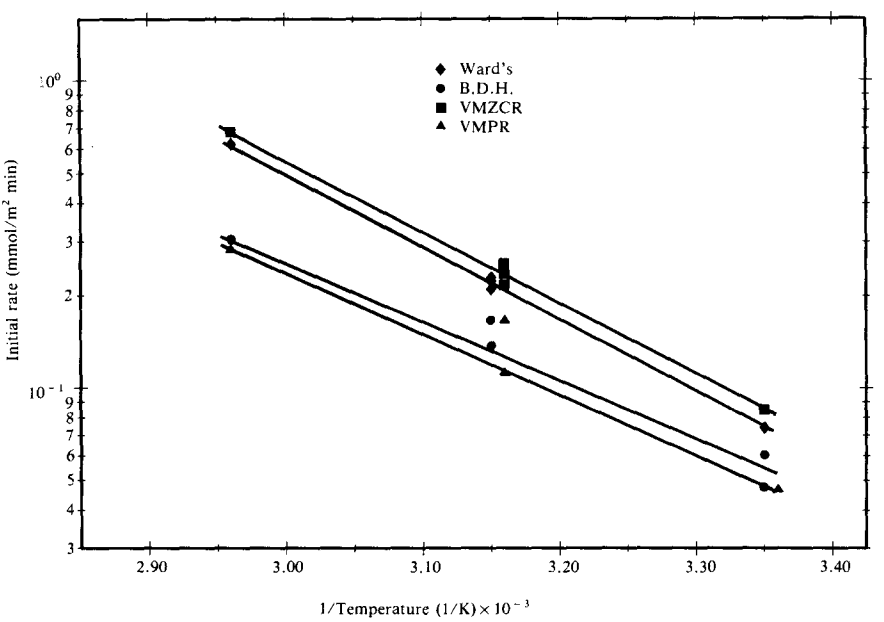

Fig. 3. Arrhenius diagram for initial rate of reaction for various sphalerites.

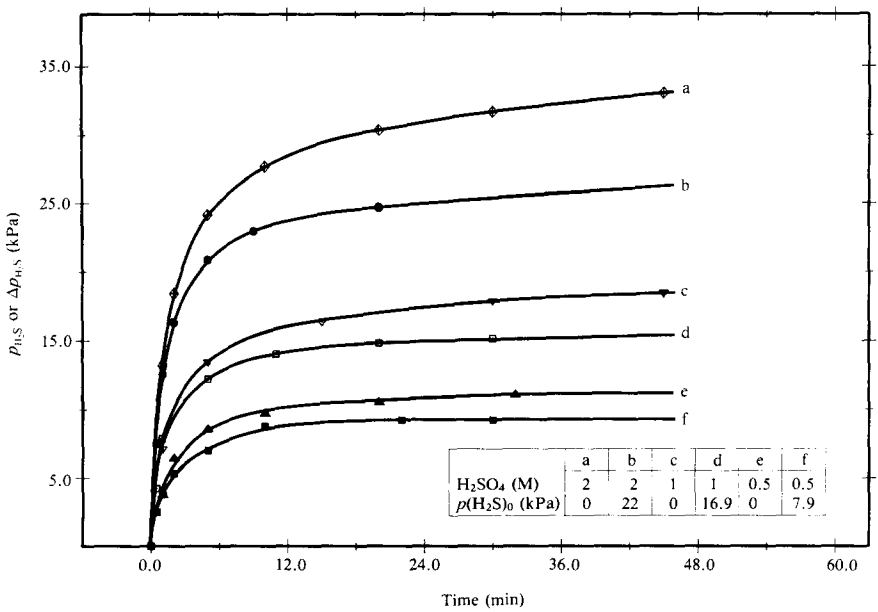

Fig. 4. Effect of $p(H_2S)_o$ on Ward's sphalerite in different concentrations of H_2SO_4 at 45 °C and a stirrer speed of 1000 min^{-1} (10 g ZnS/l).

sition reaction; therefore, since the order of dependence on $[H^+]$, α, is one,

$$k_{-1} = \frac{k_1 [H^+]_e}{[Zn^{2+}]_e^{\beta} p(H_2S)_e^{\gamma}} \tag{6}$$

where the subscript e denotes the value at equilibrium, and k_1 is determined from the slope of Fig. 2. The coefficients β and γ are determined from the logarithm of eqn. (6) and the use of a multilinear regression technique. For the Ward's, B.D.H., VMZCR, and VMPR sphalerites, values of 0.5, which are consistent with previous results [3,4], were determined for both these coefficients. The activation energies for the removal and deposition reactions are presented in Table 2.

The effect of small additions of Fe(III) on the leaching of the two pure sphalerites is shown in Figs. 6 and 7. This decrease in initial rate was also observed for various acid concentrations in the range 0.5 to 2 *M*. This effect was not observed under similar conditions for the VMZCR and VMPR sphalerites. The initial rates of reaction for VMZCR and VMPR sphalerite increased with increasing Fe(III) concentration.

The initial rate of dissolution of the impure natural sphalerites that had not been subject to vibratory milling (i.e. ZCR and PR) displayed inhibition. A comparison of the leaching behaviour of the various sphalerites for the -17 $+12$ μm size fraction is shown in Fig. 8. The dissolution of iron from these samples was also monitored. It was found that the rate of dissolution of iron

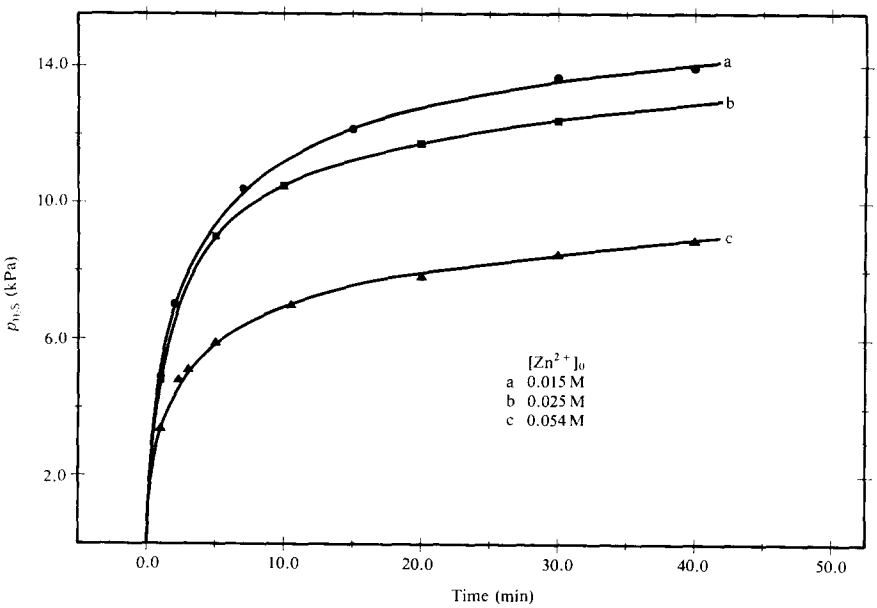

Fig. 5. Effect of $[Zn^{2+}]_0$ on Ward's sphalerite in 1 *M* H_2SO_4 at 45 °C and a stirrer speed of 1000 min^{-1} (10 g ZnS/l).

was inhibited and that the rates of dissolution of zinc and iron were similar, suggesting that the same cause of inhibition existed for the zinc and the iron. In solutions of 0.15 *M* Fe(III) containing 0.06 *M* H_2SO_4, the dissolution of these sphalerite samples was not inhibited, the reactivity of the solids increasing with increasing iron impurity in the sphalerite.

DISCUSSION

The activation energies for the removal and the deposition reactions are higher than those expected for diffusion-controlled processes (12 to 24 kJ/mol), and it is more likely that the chemical reaction is rate controlling.

TABLE 2

Activation energies for the removal and deposition reactions (eqn. 3)

Sample	Activation energy (kJ/mol)	
	Removal	Deposition
Ward's	43.9	31.6
B.D.H.	37.9	25.4
VMPR	37.4	21.1
VMZCR	44.3	30.4

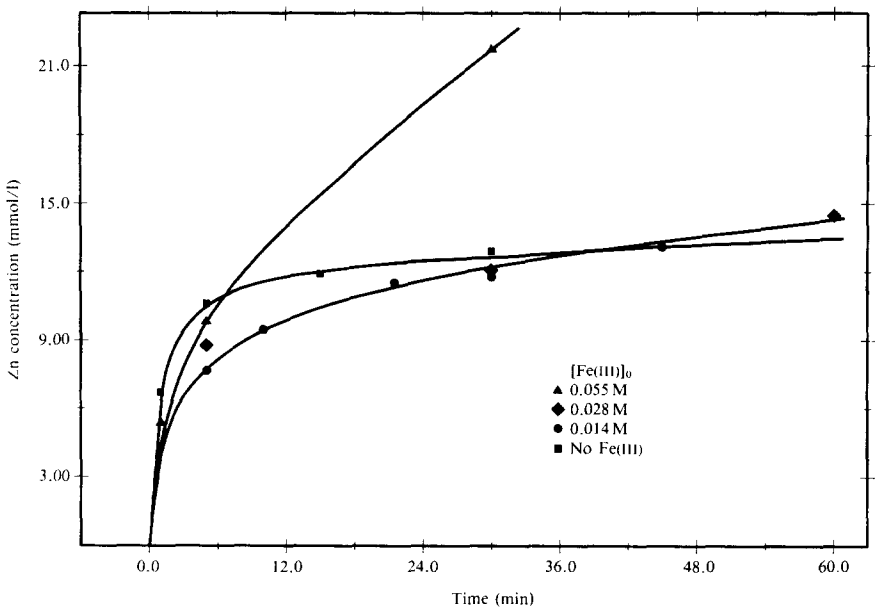

Fig. 6. Effect of $[Fe(III)]_o$ on Ward's sphalerite in 1 M H_2SO_4 at 45 °C and a stirrer speed of 1000 min^{-1} (10 g ZnS/l).

According to Vetter [1], Engell [6] and Vermilyea [5], the dissolution reaction may be governed by the transfer of ions across the Helmholtz plane. The movement of anions and cations can be treated as independent processes; therefore, for the movement of zinc lattice ions across the Helmholtz plane,

$$Zn_{lat} \rightleftharpoons Zn \tag{7}$$

the net rate of removal is given by the Butler–Volmer expression [1,5,6]

$$r_+ = \vec{k}_+ [Zn_{lat}] \exp(\alpha_+ z_+ F\phi/RT) - \overleftarrow{k}_+ [Zn] \exp\{-(1-\alpha_+) z_+ F\phi/RT\} \tag{8}$$

where ϕ is the potential across the Helmholtz plane, α_+ is the cation transfer coefficient, k represents a rate constant, and the other symbols have their usual significance. The values of the charges on the species have been omitted for purposes of simplification.

The removal of sulphur lattice ions may be followed by the complexing of protons, according to

$$S_{lat} + (a-b)\ H \rightarrow SH_{a-b} \tag{9}$$

$$SH_{a-b} + b\ H \rightleftharpoons SH_a \tag{10}$$

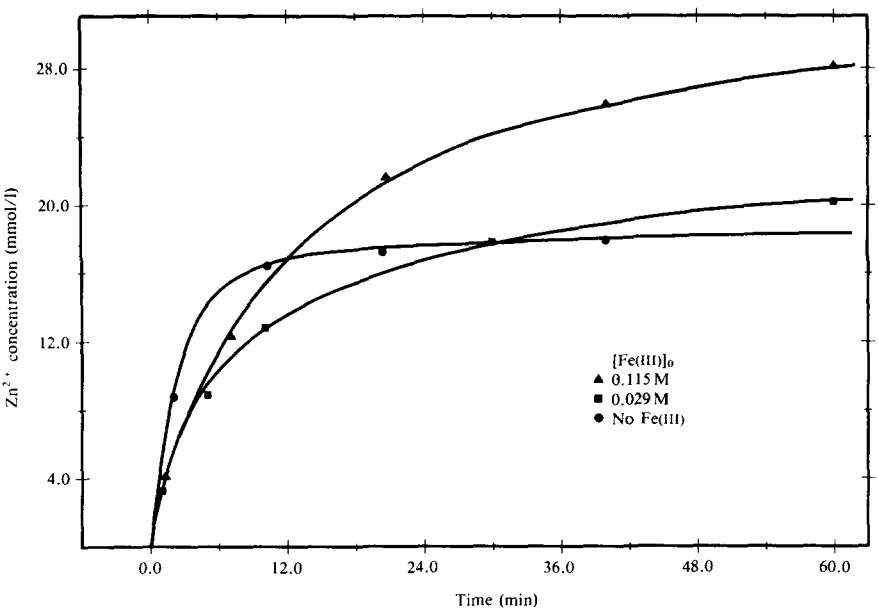

Fig. 7. Effect of [Fe(III)]$_0$ on B.D.H. sphalerite in 1 M H_2SO_4 at 45 °C and a stirrer speed of 1000 min^{-1} (4 g ZnS/l).

for which the Butler–Volmer expression [1] is

$$r_- = \vec{k}_-[S_{lat}][H]^{a-b}\exp(\alpha_- z_- F\phi/RT) - \overleftarrow{k}_-[SH_a][H]^{-b}\exp\{-(1-\alpha_-)z_- F\phi/RT\} \quad (11)$$

where a and b are stoichiometric coefficients. The freely dissolving crystal has a double-layer potential, ϕ_f, at which the net rate of removal of the cation, r_+, is equal to the net rate of removal of the anion, r_-. The initial rate is obtained by ignoring the deposition reactions, and equating the rates. This yields

$$r_o = \vec{k}_+[Zn_{lat}]\left[\frac{\vec{k}[S_{lat}][H]^{a-b}}{\vec{k}_+[Zn_{lat}]}\right]^x \quad (12)$$

where $x=\alpha_+ z_+/(\alpha_+ z_+ - \alpha_- z_-)$. The linear dependence of the initial rate on the acid concentration is obtained by assuming that each sulphide lattice ion reacts with two protons to form H_2S, i.e. $a=2$, $b=0$, $x=0.5$, which yields $\alpha_+ = \alpha_- = 0.5$.

The situation at equilibrium is described as that when the rate of removal is equal to the rate of deposition for both the cation and the anion. By setting r_+ and r_- equal to zero in eqns. (8) and (11), the following expression is obtained:

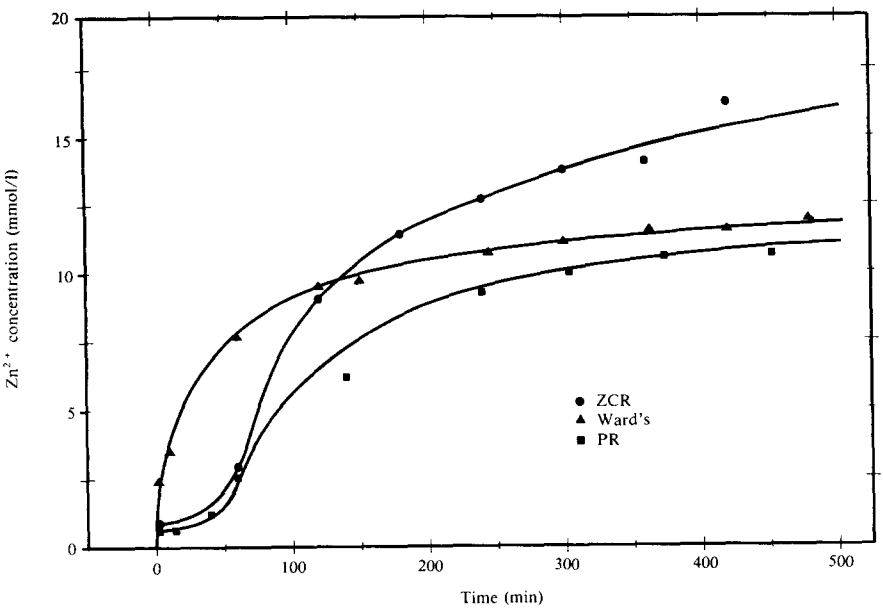

Fig. 8. Dissolution of natural sphalerites in the size fraction $-17 +12$ μm in 1 M H_2SO_4 at 45 °C and a stirrer speed of 1000 min^{-1} (BET surface area 0.42 m^2/g and 4.5 g ZnS/l for all three sphalerites).

$$\exp(z_- F\phi_e/RT) = \frac{\overleftarrow{k}_-[SH_a][H]^{-b}}{\overrightarrow{k}_-[S_{lat}][H]^{a-b}} = \frac{\overrightarrow{k}_+[Zn_{lat}]}{\overleftarrow{k}_+[Zn]} \tag{13}$$

The equilibrium constant, K, is given by

$$K = \frac{\overrightarrow{k}_+ \overrightarrow{k}_-}{\overleftarrow{k}_+ \overleftarrow{k}_-} = \frac{[SH_a][Zn]}{[H]^a} \tag{14}$$

From a comparison of eqn. (14) with the equilibrium constant for the overall reaction (eqn. (1)) and from the arguments for the initial rate dependence on $[H^+]$, it is concluded that $a=2$. Therefore eqns. (8) and (11) are the component equations for the rate eqn. (2). Equations (8) and (11) describe the initial rate and the establishment of equilibrium, that is, they are the definitive equations for the dissolution curves obtained in this study.

The addition of zinc ions to the solution in large concentrations has the effect of decreasing the initial rate, because equilibrium is established between the ions in solution and those at the surface (Fig. 5). This is verified by calculation of the equilibrium constant, i.e. $[Zn][H_2S] > 0.0001$ at 1 M H_2SO_4 as calculated from values given by Sillén [12].

Small additions of ferric ions have the effect of increasing the double-layer potential in an anodic direction, which decreases the rate. A similar effect, in which additions of Fe(III) to the solution decreased the rate, was reported by Scott and Nicol [10]. Kunieda et al. [13] observed that the rate of non-oxidative dissolution of synthetic ZnS was decreased in the presence of dissolved oxygen. Nicol [7] described results in which the dissolution of FeS, NiS, and PbS rotating-disc electrodes displayed a maximum in the curve of rate versus applied electrode potential. Figures 6 and 7 indicate that the Fe(III) also oxidizes the H_2S product (also observed in the curves of $p(H_2S)$ versus time), allowing the reaction to proceed beyond the non-oxidative equilibrium level. It was found that the presence of activated charcoal increased the level of dissolution for a similar reason.

It was assumed in the derivation of eqn. (8) that the supporting anion did not participate in the reaction. However, Majima et al. [9] have observed a first-order dependence of the rate on chloride ion at higher concentrations, and a rate that is independent of the chloride ion at low concentrations. Equation (8) is, therefore, obeyed at lower concentrations and at higher concentrations equation (8) can be rewritten in a form analogous to eqn. (11) to include the effect of the anion. Solving for the initial rate yields:

$$r_o = \vec{k}_+ [Zn_{lat}] [Cl]^{v-w} \left[\frac{\vec{k}_- [S_{lat}] [H]^{a-b}}{\vec{k}_+ [Zn_{lat}] [Cl]^{v-w}} \right]^x \tag{15}$$

To obtain first-order rate dependence on Cl^- and H^+, one assumes that two chloride ions react with a zinc ion to form the $ZnCl_2$ complex ($v-w=2$, $a-b=2$, and $x=0.5$).

Inhibition of the initial rate of dissolution of the ZCR and PR samples is shown in Fig. 8. Such inhibition has been reported for FeS [14–16] and NiO [2]. Scanning electron micrographs of particles leached in ferric ion showed that leaching does occur preferentially along grain boundaries. However, Diggle [2] concludes that changes in surface area cannot adequately account for the S-shaped curves like those of Fig. 8. The formation of surface coatings due to the presence of Pb in the ZCR sample and Cu in the PR sample would decrease the rate for the entire reaction, and would not lead to the formation of S-shaped curves.

After extensive investigation using rotating-disc electrodes, Scott and Nicol [14] proposed that for dissolution to occur, the surface of the mineral should be composed of a stoichiometric compound. In order that this can be achieved, an electron-transfer step may have to occur, followed by the non-oxidative dissolution of the stoichiometric compound. For the non-stoichiometric compound Fe_9S_{10}, they proposed that this is represented by

$$Fe_9S_{10} + 2\,H^+ + 2\,e^- \rightarrow 9\,FeS + H_2S \tag{16}$$

$$9\,FeS + 18\,H^+ \rightarrow 9\,Fe^{2+} + 9\,H_2S \quad (17)$$

and the electrons required for this reaction are supplied by the oxidation of H_2S in a mixed-potential type of process:

$$H_2S \rightarrow S^0 + 2\,H^+ + 2\,e^- \quad (18)$$

Nicol [7] has proposed a similar mechanism for Fe_3O_4. It is thought by the authors that, because a non-stoichiometric ZnS component is present in the ZCR and PR samples, an electron-transfer step is required prior to the dissolution step involving ionic charge transfer. The fact that dissolution of the same PR and ZCR samples in the presence of Fe(III) did not produce the S-shaped curves indicates that this slow electron-transfer step is the anodic oxidation of an impure ZnS. The results of the etching tests with the PR sample showed that preferential dissolution occurred in the zones of pure ZnS, suggesting that this mechanism is indeed probable. The results of the etching tests were confirmed by the S-shaped iron-dissolution curves for these experiments, since they, too, indicated that the same type of inhibition occurred for the iron component in the sphalerite. The preparation procedure, which involved washing of the sample in dilute acid, as well as the greatly increased surface area, may be the reason why there was no inhibition of the rate of dissolution of the VMZCR and VMPR samples.

CONCLUSIONS

This work has shown that the non-oxidative dissolution of sphalerite is more adequately described by an ionic charge-transfer mechanism than by previously proposed adsorption models. This mechanism is described by a Butler–Volmer expression for the removal of cations and anions from the solid lattice, and successfully describes the order of dependence of the rate on the proton concentration and the supporting anion. Locker and DeBruyn [3] found the same kinetics for ZnS, CdS, $Zn_{0.85}Cd_{0.15}S$ and ZnSe as those found in this study, indicating that this model is applicable to the non-oxidative dissolution of other group II–VI semiconductor compounds. The observed inhibition in the initial rate of reaction of the two impure natural sphalerites is explained in terms of a slow electron-transfer reaction that precedes the non-oxidative dissolution reaction.

ACKNOWLEDGEMENT

This work was conducted with financial support from the Council for Mineral Technology (MINTEK), South Africa.

LIST OF SYMBOLS

a, b	Stoichiometric coefficients, defined in eqns. (9)-(11)
A	Total surface area (m^2)
F	Faraday constant (J/V mol)
k	Rate constant
K	Equilibrium constant
K_D	Henry's law type constant
n	Number of moles H_2S or Zn^{2+} (mol)
$p(H_2S)$	Partial pressure H_2S (kPa)
r	Rate of reaction (mol/m^2 min)
R	Universal gas constant (J/mol K)
t	Time (min)
T	Temperature (K)
υ, w	Stoichiometric coefficients
V	Volume of gas or liquid
z_+, z_-	Cation, anion charge
α_+, α_-	Cation, anion transfer coefficients
ϕ	Surface–solution potential difference
Δ	Increase above initial conditions

Subscripts

e	Equilibrium conditions
f	Freely dissolving
l	Liquid
g	Gas
lat	Lattice ion, either Zn or S
o	Initial conditions
+, −	Cation, anion

Superscripts

x	Coefficient dependent on the cation and anion transfer coefficients
→, ←	Ion removal and deposition indicators
α, β, γ	Coefficients describing order of the reaction

REFERENCES

1 Vetter, K., Electrochemical Kinetics — Theoretical and Experimental Aspects, Academic Press, New York, NY, 1967.
2 Diggle, J.W. (Ed.), Oxides and Oxide Films, Marcel Dekker, New York, NY, 1973, Vol. 2, p. 281.

3 Locker, L.D. and DeBruyn, P.L., J. Electrochem. Soc., 116 (12) (1969) 1659.
4 Romankiw, L.T. and DeBruyn, P.O., in: M. Wadsworth (Ed.), Unit Operations in Hydrometallurgy, Gordon and Breach, London, 1965.
5 Vermilyea, D.A., J. Electrochem. Soc., 113 (10) (1966) 1067.
6 Engell, H.J., Z. Phys. Chem. N.F., 7 (1956) 158.
7 Nicol, M.J., in: Osseo-Asare, K. and Miller, J.D. (Eds.), Proceedings 3rd International Symposium on Hydrometallurgy, AIME, Metallurgical Society, Warrendale, PA, 1983, p. 177.
8 Pawlek, F., J.S. Afr. Inst. Min. Metall., 69 (1969) 632.
9 Majima, H., Awakura, Y. and Miskaki, N., Metall. Trans. B, 12B (1981) 645.
10 Scott, P.D. and Nicol, M.J., National Institute of Metallurgy, Report 1949, Randburg, South Africa, 1978.
11 Verbaan, B., Ph.D. Thesis, University of Natal, Durban, 1977.
12 Sillén, L.G., Stability Constants of Metal-ion Complexes, Special Publication 17, The Chemical Society, London, 1965.
13 Kunieda, Y., Samamoto, H. and Oki, T., J. Jpn. Inst. Metal., 37 (1973) 803.
14 Scott, P.D. and Nicol, M.J., National Institute of Metallurgy, Report 1858, Randburg, South Africa, 1976.
15 Scott, P.D. and Nicol, M.J., J. S. Afr. Inst. Min. Metall., 79 (1979) 298.
16 Scott, P.D. and Nicol, M.J., in: Bockris, J.O'M., Rand, D.A.J. and Welch, B.J. (Eds), Trends in Electrochemistry, Plenum, New York, NY, 1977, p. 303.